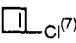


Table I. Experimental Data on Alkylchlorocarbenes

carbene	τ (exp) (ns)	τ (calc) (ns)	k_y/k_1 (M ⁻¹)	$k_y \times 10^{-9}$ (M ⁻¹ s ⁻¹)	reaction product
CH ₃ -C-Cl	330			8.86 ± 0.1	CH ₂ =CHCl ¹⁶
CH ₃ -CH ₂ -C-Cl	≈10	7.8	70	<i>a</i>	CH ₃ CH=CHCl ^{b,9}
C ₂ H ₅ -CH ₂ -C-Cl	≈10	11.7	105	<i>a</i>	C ₂ H ₅ CH=CHCl ^{b,9}
(CH ₃) ₂ CH-C-Cl	≈10	11.3	125	11 ± 3	(CH ₃) ₂ C=CHCl ⁹
Ph-CH ₂ -C-Cl	16.5			7.5 ± 0.5	Ph-CH=CHCl ^{b,9}
Ph-CH(CH ₃)-C-Cl	<3	≈1.5	13	<i>a</i>	Ph-C(CH ₃)=CHCl ^{b,10}
(CH ₃) ₃ C-C-Cl	≈90 ¹¹			2.4 ± 0.2	(CH ₃) ₂ C=C(CH ₃)Cl ⁹
c-C ₃ H ₅ -C-Cl	1670			0.47 ± 0.3	 Cl ⁽⁷⁾
	2600 ^c				

^a Assumed to be equal to 9×10^9 M⁻¹ s⁻¹, mean value of the three k_y values measured for >CH-C-Cl type carbenes. ^b Z and E isomers are produced: $k_1 = 1/\tau$ represents an average for the two competing H-shifts. ^c From the direct observation of the carbene decay at 250 nm, after correction for a second-order process which significantly shortens the apparent lifetime of this carbene as measured by the pyridine ylide technique. The second-order process (dimerization) is important in this case because the carbene concentrations produced in LFP are large and the rearrangement to cyclobutene is particularly slow.

Table II. Calculated Activation Parameters E_a (kcal/mol) and ΔS^\ddagger (cal/mol·K)

carbene	hydrogen migration			methyl migration	
	E_a^{MNDO}	$E_a^{\text{MINDO/3}}$	$\Delta S^\ddagger \text{ MNDO}$	E_a^{MNDO}	$E_a^{\text{MINDO/3}}$
CH ₃ -C-Cl	30.3	9.4	-3.5		
CH ₃ -CH ₂ -C-Cl	28.2	6.0	-3.1	37.6	15.4
(CH ₃) ₂ CH-C-Cl	24.5	2.5	-3.8		
(CH ₃) ₃ C-C-Cl				29.0	1.0
Ph-CH ₂ -C-Cl	26.1	4.3	-3.6		
Ph-CH(CH ₃)-C-Cl	22.8	2.3			

and isopropylchlorocarbenes because of the short lifetime of these species: with low [pyridine], the yield of ylide formation is low, and therefore the measured absorptions are weak; with high [pyridine], k_{growth} is so large that it cannot be measured accurately with our setup. In Ph-CH(CH₃)-C-Cl, the 1,2-H migration is so fast that the determination of k_1 by this method is beyond the capability of our detection system. In these cases, the ratio k_y/k_1 has been determined from the linear plots of 1/OD vs 1/[pyridine] with OD being the absorbance of the ylide. Assuming that k_y is very similar for all these carbenes and close to 9×10^9 M⁻¹ s⁻¹, the values for $\tau = 1/k_1$ can be calculated (τ (calc) in Table I) for the alkylchlorocarbenes and for Ph-CH(CH₃)-C-Cl.

Activation parameters calculated by MNDO and MINDO/3 methods are presented in Table II. By using configuration interaction we find that, in the case of CH₃-C-Cl, the triplet surface does not play a role in the 1,2 H migration. Therefore the calculations have been performed for all carbenes at the singlet RHF level along the reaction path, in the same way as in ref 12. The geometries for the stationary points (carbene and transition state) are fully optimized. The calculated ΔS^\ddagger are similar for all carbenes suggesting that the difference in carbene lifetimes is due to their respective E_a . Both methods indicate that the E_a are running parallel to the experimental migratory aptitudes. A known deficiency of MNDO is that it disfavors nonclassical structures, producing high E_a for migrations. On the other hand, MINDO/3 which favors small rings¹³ (such as the transition state for the 1,2-H migration) gives more realistic values for barriers to rearrangement, e.g., the calculated E_a for rearrangement in Ph-CH₂-C-Cl is in excellent agreement with the experimental values of 6.4⁹ and 4.5¹⁴ kcal/mol.

It is clear from the present results that 1,2-H migration is enhanced by substitution on the α -carbon. Thus, the hydrogen migration in (CH₃)₂CH-C-Cl is 30 times faster than in C-H₃-C-Cl, and in Ph-CH(CH₃)-C-Cl it is 10 times faster than in Ph-CH₂-C-Cl. Since electronic effects are cumulative as shown in our calculations, we find it surprising that the H migratory aptitudes are similar in CH₃-CH₂-C-Cl, C₂H₅-CH₂-C-Cl, and (CH₃)₂CH-C-Cl. This suggests either that the maximum enhancement in rate is reached by the addition of one methyl group

on the α -position or the occurrence of an alternative reaction pathway.

It is generally accepted that hydrogen migration is faster than methyl migration. This is confirmed by the fact that only 1,2-H shifts are observed for CH₃-CH₂-C-Cl. However, we must be cautious when comparing the 1,2-H shift and the 1,2 alkyl shift between carbenes in the same series: for example, the methyl shift in (CH₃)₃C-C-Cl is three times faster than the hydrogen shift in CH₃-C-Cl due to the inductive effects of the methyl groups. The 1,2 migration of the cyclopropyl C-C bond in c-C₃H₅-C-Cl to give 1-chlorocyclobutene is particularly interesting. Moss and Fantina⁷ have argued that the efficient intermolecular capture of c-C₃H₅-C-Cl is due to an increased stability of this carbene. Our observed rate constants for this series certainly support this idea.

Experimental determination of activation parameters for alkylchlorocarbenes is underway.

Ligand Oxidation in a Nickel Thiolate Complex

Manoj Kumar, Roberta O. Day, Gerard J. Colpas, and Michael J. Maroney*

Department of Chemistry, University of Massachusetts
Amherst, Massachusetts 01003
Received April 3, 1989

Recent interest in the factors that stabilize formally Ni(III) sites in many hydrogenases (H₂ases) and carbon monoxide dehydrogenases has stimulated investigations of Ni(II) thiolates.¹⁻⁵ Studies of the redox chemistry of Ni(II) complexes reveal that oxidations to Ni(III) or reductions to Ni(I) typically occur at potentials outside those accessible in biological systems.⁶⁻⁸ Coordination environments incorporating thiolate ligands might be expected to stabilize Ni(III); however, recent studies suggest that ligand oxidation leading to the formation of disulfides may occur in preference to metal oxidation.¹ Detailed knowledge of these redox processes is important in understanding the mechanism(s) involved in small-molecule activation in the metalloenzymes and is currently limited by the paucity of well-characterized oxidation products. We report the first study of the oxidation of nickel thiolates involving three oxidation levels where the initial and final

(11) Jackson, J. E.; Soundararajan, N.; Platz, M. S.; Liu, M. T. H. *J. Am. Chem. Soc.* **1988**, *110*, 5595.

(12) Frenking, G.; Schmidt, J. *Tetrahedron* **1984**, *40*, 2123.

(13) Kyba, E. P. *J. Am. Chem. Soc.* **1977**, *99*, 8330.

(14) Measurement by laser flash photolysis to be published.

(1) Krüger, H.-J.; Holm, R. H. *Inorg. Chem.* **1989**, *28*, 1148-1155.

(2) Krüger, H.-J.; Holm, R. H. *Inorg. Chem.* **1987**, *26*, 3645-3647.

(3) Rosenfield, S. G.; Armstrong, W. H.; Mascharak, P. K. *Inorg. Chem.* **1986**, *25*, 3014-3022.

(4) Rosenfield, S. G.; Berends, H. P.; Gelmini, L.; Stephan, D. W.; Mascharak, P. K. *Inorg. Chem.* **1987**, *26*, 2792-2797.

(5) Saint-Martin, P.; Lespinat, P. A.; Fauque, G.; Berlier, Y.; LeGall, J.; Teixeira, M.; Xavier, A. V.; Moura, J. J. G. *Proc. Natl. Acad. Sci. U.S.A.* **1988**, *85*, 9378-9380.

(6) Haines, R. I.; McAuley, A. *Coord. Chem. Rev.* **1981**, *39*, 77-119.

(7) Nag, K.; Chakravorty, A. *Coord. Chem. Rev.* **1980**, *33*, 87-147.

(8) Teixeira, M.; Moura, I.; Xavier, A. V.; Huynh, B. H.; DerVartanian, D. V.; Peck, H. D., Jr.; LeGall, J.; Moura, J. J. G. *J. Biol. Chem.* **1985**, *260*, 8942-8950.

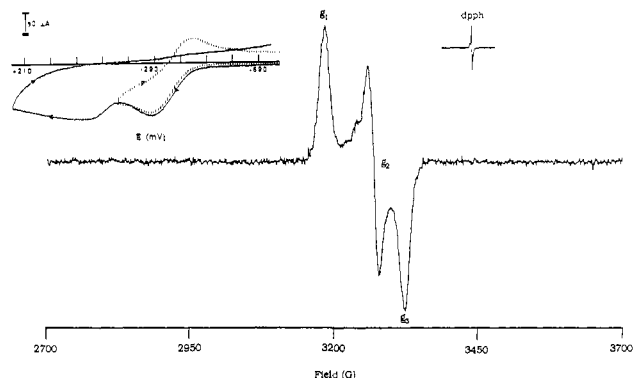
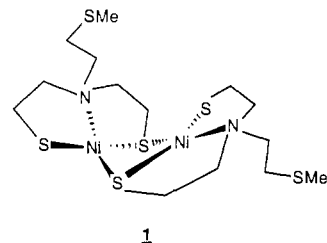


Figure 1. Frozen-solution (77 K) X-band EPR spectrum ($\nu = 9.60$ GHz) obtained for the product of electrochemical reduction of **1** at -190 mV (g values are 2.17, 2.11, and 2.07). Inset: Cyclic voltammograms of $[\text{Ni}(\text{NS}_2\text{SMe})_2]_2$, 1 mM in 0.1 M $n\text{-Bu}_4\text{N}(\text{ClO}_4)\text{-CH}_2\text{Cl}_2$ solution. Sweep rate = 250 mV/s. Potentials are referenced to internal ferrocene/ferricinium.¹³

complexes are structurally characterized. These studies demonstrate that thyl radicals are intermediates in the oxidative process.

Reaction of N,N -bis(2-mercaptoethyl)-2-(methylthio)ethylamine (NS_2SMe)⁹ (100 mg, 47 mmol) with anhydrous $\text{Ni}(\text{OAc})_2$ (84 mg, 47 mmol) at 5°C in MeOH yields the black dimeric product $[\text{Ni}(\text{NS}_2\text{SMe})_2]_2$ (**1**) in 65% yield.¹⁰ The crystal structure



1

of the dimer is represented by **1**¹¹ and is similar to the structures of analogous systems.¹² Two oxidations with anodic peak potentials at -290 and -30 mV were observed for the dimer by cyclic voltammetry (Figure 1).¹³ When the scan is reversed at -140 mV, the first oxidation becomes pseudoreversible with the appearance of a cathodic peak at -410 mV. Controlled-potential electrolysis of cold CH_2Cl_2 solutions (-35 to -40°C) at -190 mV yields a one-electron oxidation product (coulometric analysis, 0.80 electron/dimer). During the 40-min oxidation, a green solution is produced that gives the EPR spectrum shown in Figure 1 at 77 K with g values of 2.17, 2.11, and 2.07. These g values and the lack of ^{14}N hyperfine are features that show a striking similarity to those associated with various $S = 1/2$ Ni species in H_2 ases.¹⁴ Integration of the EPR signals yields spin concentrations that agree within 2% with the number of electrons transferred. Cyclic voltammograms taken of the electrolyzed product (at -35 to -40°C) do not reveal any new features, indicating that the oxidation is chemically reversible and that the oxidized species is a dimer. The one-electron oxidation product has limited stability

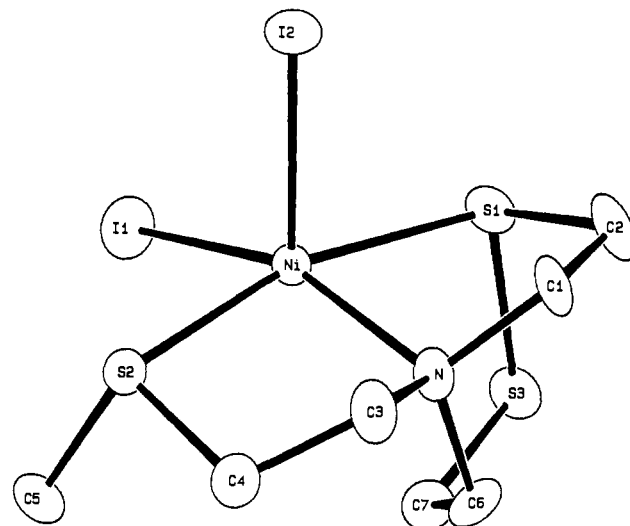


Figure 2. ORTEP plot of **2** with thermal ellipsoids at the 30% probability level. Selected bond distances in angstroms are Ni-S1, 2.407 (4); Ni-S2, 2.377 (4); Ni-N, 2.109 (10); Ni-I1, 2.620 (2); Ni-I2, 2.627 (2); and S1-S3, 2.056 (5). Selected bond angles in degrees are I1-Ni-I2, 104.0 (1); I1-Ni-S1, 94.2 (1); I1-Ni-S2, 93.9 (1); I1-Ni-N, 154.1 (3); I2-Ni-S1, 92.4 (1); I2-Ni-S2, 97.8 (1); I2-Ni-N, 101.6 (3); S1-Ni-S2, 165.0 (1); S1-Ni-N, 81.0 (3); S2-Ni-N, 86.3 (3); Ni-S1-S3, 98.4 (2).

at room temperature. Solutions electrolyzed for 30 min at room temperature display an EPR signal that integrates to 10–15% of the expected amount of product.

Chemical oxidation of **1** with I_2 in CHCl_3 leads to the immediate loss of the purple color of I_2 and the formation of a dark brown microcrystalline solid, $\text{Ni}(\text{NS}_2\text{SMe})_2$ (**2**), in 84% yield.¹⁵ Magnetic susceptibility measurements¹⁹ of **2** reveal $\mu = 2.80 \mu\text{B}$ at 293 K, a value that is indicative of a high-spin ($S = 1$) Ni(II) center. The structure of **2**¹⁶ (Figure 2) reveals that a four-electron oxidation of **1** has occurred, leading to the formation of a distorted square-pyramidal Ni(II) complex with a disulfide ligand. Intramolecular coupling of two thyl radicals is apparently involved in the formation of the disulfide, which is contained in a seven-membered ring that also contains the N-donor atom. Oxidation of coordinated thiolates has been reported in several systems,^{17,18} and the isolation and spectroscopic characterization of cyclic disulfides similar to that in **2** have also been reported.¹⁷ However, few Ni disulfide complexes have been structurally characterized.¹⁸

Structural investigations of H_2 ases using X-ray absorption spectroscopy reveal that the Ni sites in these enzymes are 5- to 6-coordinate and are bound to at least two S-donor ligands.²⁰ EPR studies of the Ni sites of various H_2 ases confirm the role of sulfur ligands²¹ and reveal $S = 1/2$ Ni species associated with oxidized and reduced enzymes.¹⁴ The appearance and disappearance of these EPR signals during redox cycling of the enzymes have been

(15) Anal. ($\text{Ni}_2\text{H}_{15}\text{NS}_3\text{I}_2$): C, H, N, I.

(16) X-ray analysis of **2**: Crystals from DMF/ether, monoclinic space group $P2_1/n$, $a = 8.888$ (1) Å, $b = 12.729$ (3) Å, $c = 12.746$ (3) Å, $\beta = 96.25$ (1)°, $V = 1433.5$ (9) Å³, $Z = 4$. The present values of $R = 0.038$ and $R_w = 0.042$ are based on anisotropic unit-weighted refinement of non-hydrogen atoms. The structure was solved by use of the heavy-atom method. Full details will be published elsewhere.

(17) Stein, C. A.; Taube, H. *Inorg. Chem.* **1979**, *18*, 2212–2216.

(18) (a) Warner, L. G.; Kadooka, M. M.; Seff, K. *Inorg. Chem.* **1975**, *8*, 1773–1778. (b) Warner, L. G.; Ottersen, T.; Seff, K. *Inorg. Chem.* **1974**, *13*, 2529–2534. (c) Riley, P. E.; Seff, K. *Inorg. Chem.* **1972**, *11*, 2993–1006.

(19) Performed with a Johnson-Matthey susceptibility balance, error in measurement $< \pm 2\%$, corrected for diamagnetic contributions.

(20) (a) Eidsness, M. K.; Scott, R. A.; Pickril, B. C.; DerVartanian, D. V.; LeGall, J.; Moura, I.; Moura, J. J. G.; Peck, H. D., Jr. *Proc. Natl. Acad. Sci. U.S.A.* **1989**, *86*, 147–151. (b) Eidsness, M. K.; Sullivan, R. J.; Scott, R. A. In *The Bioinorganic Chemistry of Nickel*; Lancaster, J. R., Ed.; VCH Publishers: New York, 1988; Chapter 4. (c) Lindahl, P. A.; Kojima, N.; Hausinger, R. P.; Fox, J. A.; Teo, B. K.; Walsh, C. T.; Orme-Johnson, W. H. *J. Am. Chem. Soc.* **1984**, *106*, 3062–3064.

(21) Albracht, S. P. J.; Kröger, A.; van der Zwaan, J. W.; Uden, G.; Böcher, R.; Mell, H.; Fontijn, R. D. *Biochim. Biophys. Acta* **1986**, *874*, 116–127.

(9) Corbin, J. L.; Miller, K. F.; Pariyadath, N.; Wherland, S.; Bruce, A. E.; Stiefel, E. I. *Inorg. Chim. Acta* **1984**, *90*, 41–51.

(10) Anal. ($\text{Ni}_2\text{C}_{14}\text{H}_{30}\text{N}_2\text{S}_6$): C, N; H, calcd 5.64, found 5.03.

(11) Kumar, M.; Day, R. O.; Colpas, G. J.; Maroney, M. J., manuscript in preparation.

(12) (a) Baker, D. J.; Goodall, D. C.; Moss, D. S. *Chem. Commun.* **1969**, 325. (b) Villa, A. C.; Manfredotti, A. G.; Nardelli, M.; Pelizzi, C. *Chem. Commun.* **1970**, 1322–1323. (c) Wei, C. H.; Dahl, L. F. *Inorg. Chem.* **1970**, *9*, 1878–1887.

(13) Cyclic voltammetry: 1 mM solution of **1** in 0.1 M $n\text{-Bu}_4\text{N}(\text{ClO}_4)/\text{CH}_2\text{Cl}_2$, using a glassy carbon working electrode, Pt wire auxiliary electrode, and Ag wire pseudo reference electrode. All potentials are referenced to internal ferrocene/ferricinium, which has a value of $+400$ mV vs NHE. See: Gagne, R. R.; Allison, J. L.; Gall, R. S.; Koval, C. A. *J. Am. Chem. Soc.* **1977**, *99*, 7170–7177.

(14) (a) Cammack, R.; Fernandez, V. M.; Schneider, K. In *The Bioinorganic Chemistry of Nickel*; Lancaster, J. R., Ed.; VCH Publishers: New York, 1988; Chapter 4. (b) Moura, J. J. G.; Teixeira, M.; Moura, I.; LeGall, J. *Ibid.*, Chapter 9.

interpreted by using a variety of schemes involving Ni(III)/Ni(II),^{8,14b} Ni(III)/Ni(II)/Ni(I),^{14a} and Ni(III)/Ni(II)/Ni(I)/Ni(0)²² formal oxidation states. In all these schemes, the assignment of Ni(III) to the oxidized forms of the enzymes is based on the observation of hyperfine in ⁶¹Ni-labeled enzymes, the similarity of the EPR spectra to EPR spectra of tetragonal Ni(III) coordination compounds, and the association of the signal with oxidized forms of the enzymes. The studies outlined here suggest that Ni(III) has no real existence in systems with simple alkyl thiolate ligation. From the viewpoint of ligand oxidation, the "Ni(III)" EPR signal could be interpreted as arising from a tetragonal *S* = 1, Ni(II) center with the spin in the *d*_{x²-y² orbital antiferromagnetically coupled to a thiyl radical. The resulting *S* = 1/2 system (with an unpaired spin in the *d*_{z² orbital) is consistent with the observed EPR spectrum and with the small Ni K-edge shifts observed in XAS spectra,^{20b} is more consistent with known Ni thiolate redox chemistry, and suggests that nature may have selected a *non-redox-active* metal (Ni) for these roles in order to stabilize ligand-based redox chemistry.}}

Acknowledgment. We gratefully acknowledge funding in support of this research from NIH Grant GM-38829.

Supplementary Material Available: Tables of positional and thermal parameters for **2** (2 pages). Ordering information is given on any current masthead page.

(22) van der Zwaan, J. W.; Albracht, S. P. J.; Fontijn, R. D.; Slater, E. C. *FEBS Lett.* **1985**, *179*, 271-277.

Self-Assembling Ionophores

Alanna Schepartz* and Jason P. McDevitt

*Sterling Chemistry Laboratory
Yale University, 225 Prospect Street
New Haven, Connecticut 06511-8118
Received March 22, 1989*

One of the mechanisms by which enzyme active sites are formulated is through the assembly of subunits, which alone are incapable of substrate recognition.¹ Enzymes such as phosphofructokinase² and aspartate transcarbamoylase³ exhibit this property, as do organelles such as the ribosome. In each case, the association and dissociation of a subunit regulates the biological event, whether that event is phosphorylation of fructose 6-phosphate or the biosynthesis of a polypeptide. The systems designed by Rebek,⁴ Shinkai,⁵ and Irie⁶ have demonstrated the ability to tailor a conformational change in a single molecule to induce a chemical event. However, the *assembly* of a *functioning* binding unit from two discrete molecules has remained a phenomenon reserved exclusively for high molecular weight systems.^{7,8} In this

(1) Hammes, G. G. *Enzyme Catalysts and Regulation*; Academic: New York, 1982; Chapter 8. Huang, C. Y.; Rhee, S. G.; Chock, P. B. *Ann. Rev. Biochem.* **1982**, *51*, 935-971.

(2) Lau, F. T.-K.; Fersht, A. R. *Nature* **1987**, *326*, 811-812. Evans, P. R.; Hudson, P. J. *Nature* **1979**, *279*, 500-504.

(3) Wente, S. R.; Schachman, H. K. *Proc. Natl. Acad. Sci. U.S.A.* **1987**, *84*, 31-35.

(4) Rebek, J., Jr.; Costello, T.; Marshall, L.; Wattlely, R.; Gadwood, R. C.; Onan, K. J. *Am. Chem. Soc.* **1985**, *107*, 7481-7487, and references cited therein.

(5) Shinkai, S.; Miyazaki, K.; Manabe, O. *J. Chem. Soc., Perkin Trans. II* **1987**, 449-456, and references cited therein.

(6) Irie, M.; Kato, M. *J. Am. Chem. Soc.* **1985**, *107*, 1024-1028.

(7) Self-assembly as a strategy is not new; some recent examples follow. Cytotoxins: Rideout, D. *Science* **1986**, *233*, 361-363. Porphyrins: Traylor, T. G.; Mitchell, M. J.; Ciccone, J. P.; Nelson, S. J. *Am. Chem. Soc.* **1982**, *104*, 4986-4989. Tabushi, I. *Pure Appl. Chem.* **1988**, *60*, 581-586. Surfaces: Bain, C. D.; Troughton, E. B.; Tao, Y. T.; Evall, J.; Whitesides, G. M.; Nuzzo, R. G. *J. Am. Chem. Soc.* **1989**, *111*, 321-325. Inorganic helices: Lehn, J.-M.; Rigault, A.; Siegel, J.; Harrowfield, J.; Chevrier, B.; Moras, D. *Proc. Natl. Acad. Sci. U.S.A.* **1987**, *84*, 2565-2569. Paramagnetic shift reagents: Gupta, R. K.; Gupta, P. *J. Magn. Reson.* **1982**, *47*, 344-350.

(8) An example of assemblage of a binding site for ammonium ions using hydrogen bonds has been reported: Kim, M.; Gokel, G. W. *J. Chem. Soc., Chem Commun.* **1987**, 1686-1688.

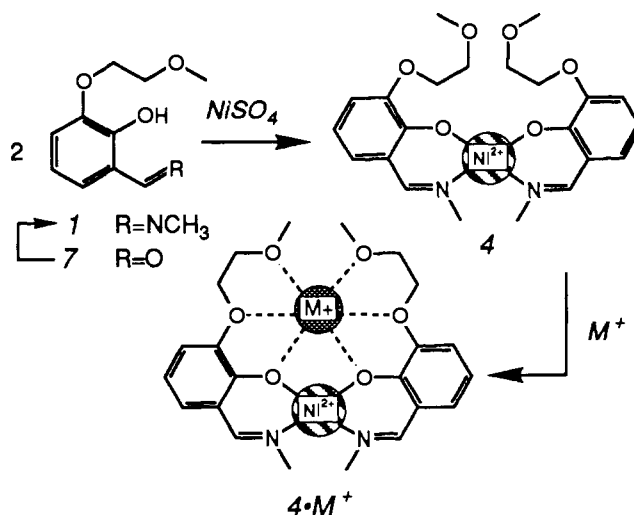


Figure 1.

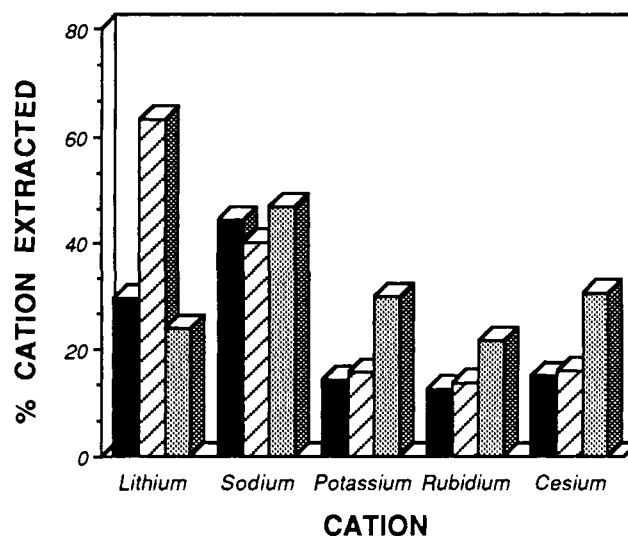


Figure 2. Extent of alkali metal ion extraction by complexes **4**, **5**, and **6**, at 25 ± 5 °C. Aqueous phase: [M⁺Picrate] = 7.5 mM. Chloroform phase: [host] = 2 mM. Values are averages of at least two independent determinations. All values are reproducible to within 5%.

communication we demonstrate that this phenomenon may be reproduced using small molecules.

Simple, linear polyethers with fewer than four oxygen atoms do not bind alkali metal ions tightly and are unable to transport those ions across membranes with high efficiency.⁶ Binding is enthalpically disfavored by the lack of suitable ligand sites. Dimerization of two polyethers would generate the requisite number of binding sites; however, the concomitant loss in entropy is so great that it overrides any enthalpic gain.⁹ We report herein that Ni(II) can act as a *template* to permit the assembly of dimeric, cation-selective inclusion complexes from imines **1**, **2**, and **3**.¹⁰ The resulting complexes **4**, **5**, and **6**¹¹ are able to extract alkali metal ions efficiently from aqueous solution with selectivities

(9) Tümmeler, B.; Maass, G.; Vögtle, F.; Sieger, H.; Heimann, U.; Weber, E. *J. Am. Chem. Soc.* **1979**, *101*, 2588-2598.

(10) Prepared by monoalkylation of 2,3-dihydroxybenzaldehyde with the appropriate bromide and condensation with methylamine. van Stavaren, C. J.; van Eerden, J.; van Veggel, F. C. J. M.; Harkema, S.; Reinhoudt, D. N. *J. Am. Chem. Soc.* **1988**, *110*, 4994-4508.

(11) Prepared by reaction with NiSO₄ as described by Holm: Holm, R. H.; O'Connor, M. J. *Prog. Inorg. Chem.* **1971**, *14*, 241-401. The green, paramagnetic complexes were purified by recrystallization from cyclohexane and characterized by elemental analysis and UV-vis spectroscopy. All complexes are monomeric in chloroform solution, as judged by vapor pressure osmometric studies at 25 °C. Osmometry was performed by Schwarzkopf Microanalytical Laboratory, Woodside, NY 11377. Since the three-dimensional structures of these complexes are not yet available, Figures 1 and 3 illustrate only hypothetical structures.